JOURNAL OF SPACECRAFT AND ROCKETS
Vol. 34, No. 3, May–June 1997

Solid Rocket Motor Exhaust Model for Alumina Particles in the Stratosphere

Edward J. Beiting*
The Aerospace Corporation, El Segundo, California 90245

Based on available and new data, a unified model is presented for the particle size distribution, particle density, and geometrical dispersion for the alumina particles in the exhaust of solid rocket motor plumes in the stratosphere. The particle size distribution is trimodal with Sauter mean diameters of 0.056, 1.0, and 3.6 μm. Nearly all of the particles lie within the small-size mode but nearly all of the mass lies in the large-size mode. Approximately two-thirds of the particle surface area available for heterogeneous chemical reactions is due to the large particle mode while most of the remaining surface area is due to the small particle mode. The early horizontal dispersion rate of the plume is found to be about an order of magnitude greater than the dispersion rates used in several recent models of stratospheric ozone-plume chemistry.

Nomenclature

A_p = cross-sectional area of plume, m^2
a = geometrical cross-sectional area of particle, cm^2
a_{tot} = total surface area of all particles per unit volume of air, $\mu m^2\ cm^{-3}$
b = diffusivity scale parameter, $m\ s^{-1}$
C_m = mass of particle per volume of air, $g\ cm^{-3}$
D = particle diameter, μm
D_{32} = Sauter mean diameter of particle, μm
K_{yy} = horizontal diffusion coefficient, $m^2\ s^{-1}$
K_{zz} = vertical diffusion coefficient, $m^2\ s^{-1}$
L = path length through plume, m
M_L = total mass of alumina exhausted from solid rocket motor per vehicle track length, $g\ m^{-1}$
$n(t)$ = particle number density, cm^{-3}
n_0 = initial particle number density, cm^{-3}
$p(z)$ = atmospheric pressure, mbar
R_i = initial plume radius, m
r = radial coordinate in plume, m
V = volume of particle, μm^3
v_{tot} = total volume of particle per unit mass of air, $\mu m^3\ cm^{-3}$
z = altitude coordinate, m
γ = particle mode parameter, μm^{-1}
$\rho(D)$ = mass density of alumina particle, $g\ cm^{-3}$

Introduction

THE environmental effects of solid rocket motor (SRM) exhaust on the atmosphere have been the topic of much recent interest. There is general agreement that the atmospheric effects of exhaust of large SRMs (Titan, Shuttle, Ariane) at current and projected launch rates[1] are small compared to total global anthropogenic impacts (although comparable to some other industrial sources).[2,3] However, the local effects of SRM exhaust on the stratospheric ozone layer are predicted to be significant. In particular, models predict that after burning in the plume converts HCl to more active forms of chlorine, which create a transient ozone hole.[4–13] The size and persistence of the reduced O_3 concentrations is a sensitive function of the assumed chemistry, alumina (Al_2O_3) particle characteristics, and especially the plume dispersion rate. Other than a brief mention of depressed ozone levels of a plume fly-through, which indicated a 40% decrease in ozone concentration about 15 min after vehicle passage, no observational evidence exists of this effect.[14] [Note: A program called Rocket Impact of Stratospheric Ozone (RISO) sponsored by the U.S. Air Force is currently collecting data using LIDAR and aircraft penetrating SRM plumes in the stratosphere to study this subject.] Consequently, the ability to verify experimentally the predictions of these models has become a topic of considerable discussion.[15–21]

Many of the proposed techniques for these verification measurements are optical. The ability to interpret the data collected by these instruments and even the projection of the feasibility of the techniques themselves depend on an a priori knowledge of the characteristics of the alumina particles in the plume. Additionally, the particles may play a role in the chemical interaction of the plume through heterogeneous reactions.[22–24] Understanding the effects of the heterogeneous chemistry requires knowledge of the total particle area available as a reaction surface in addition to gas-particle adsorption/desorption kinetics and the number density of the gaseous chemical constituents of the plume.

This work attempts to address these needs by gathering the best available data on SRM exhaust particles and plume dispersion in the stratosphere. This information is used to develop a model of specific particle density, that is, the particle number density as a function of particle size, altitude, position in the plume, and time after vehicle passage. The model is presented for a Titan IV vehicle but is easily scaled to any of the large SRMs in use. Estimates of the reaction surface area and other physical characteristics of the plume then are predicted based on this model. In a companion publication,[25] this model is used to predict optical properties of an SRM plume in the stratosphere.

Particle Characteristics of an SRM Plume

In this section, we identify the sources of SRM plume particle data, review the characteristics of the particles in the plume, and define a particle size distribution. Particle size measurements have been made in the motors of subscale rockets,[26–30] in the ground clouds of a Titan[31,32] and the Space Shuttle,[33] in the upper tropospheric plume of the STS,[33–36] in the stratospheric plume of a Titan,[32] and in the plume of an Atlas.[31] Particle density measurements were made in the tropospheric plumes of the STS[34,36] and the ground cloud[31,32] and stratospheric plume[32] of a Titan. Particle morphology was studied in the ground clouds of a Titan[32] and the STS,[33] in the stratospheric plumes of a Titan,[32] and the tropospheric plumes of the STS.[33,35–37] Chemical composition was studied of the particles collected in stratospheric plumes of a Titan[32] and the tropospheric plumes of the STS,[37] as well as from plumes of other small rockets (PAM D-II, IUS, Peacekeeper Stage II).[38] Studies of the environmental effects of particles from STS plumes in the troposphere[39] and stratosphere[39,40] have also been made. Some relevant results from these works are as follows.

1) The particle size distribution extends from below 0.03 μm to approximately 10 μms and may be trimodal in the stratosphere in

Received June 20, 1996; presented as Paper 97-0532 at the 35th Aerospace Sciences Meeting, Reno, NV, Jan. 6–10, 1997; revision received Feb. 8, 1997; accepted for publication Feb. 11, 1997.

*Research Scientist, P.O. Box 92957, Los Angeles, CA 90009-2957. Member AIAA.

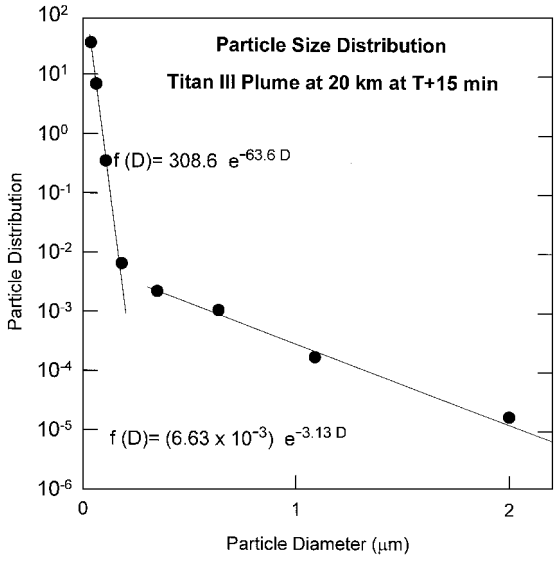

Fig. 1 Fits to stratospheric Titan III plume data of Strand et al.[32]

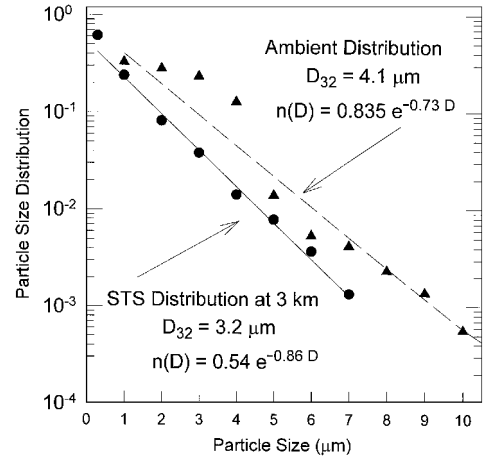

Fig. 2 Fits to ambient stratospheric particle data of Zolensky et al.[44] and tropospheric STS plume particle data of Cofer et al.[36]

this size range for large rockets.[32,37] At stratospheric altitudes, particle size increases with time (during the first few minutes after vehicle passage) for particles with diameters between 0.3 and 1.33 μm due to condensation of vapors or agglomeration.[32] Particle size decreases with increasing rocket motor size.[28]

2) The particles are spherical in shape and have a composition of Al_2O_3 with trace amounts of other elements (K, Na, Ti, Fe, Si) and small surface contamination of HCl.[32,35–37,39] The density of the particles varied between 1.5 and 3.5 g cm^{-3}, with larger particles tending to have lower densities (presumably because they are hollow or porous).[32,39]

3) Most of the Al_2O_3 is cubic gamma phase, and the ratio of gamma to hexagonal alpha phase is about four.[38] The small particles tend to be in the gamma phase.[41]

4) In the troposphere between 3 and 7 km, the particle size distribution is independent of altitude for particles with diameters greater than 1 μm (Ref. 36).

5) Initially the particle size distribution is a function of radial position in the plume. The smallest particles are uniformly distributed, but the larger particles are confined to the plume center.[29] Nozzle/plume flowfield codes predict that particles larger than 1 μm are concentrated along the plume centerline, and particles as small as 1 μm cannot follow the flow along the diverging nozzle wall.[42,43]

There is only one report of in-situ observations of particle size distribution and density of large SRMs (Titan IIIs) in the stratosphere.[32] These measurements were restricted to particle diameters below 2 μm and were taken using two different types of instruments (oil wire impactor and sticky tape). Both instruments measured identical distributions. The sticky tape measurements are plotted in Fig. 1, where we fit them to exponential functions. The distribution is clearly bimodal, and we calculate Sauter mean diameters of 0.056 and 1.0 μm and slopes of 63.6 and 3.13, respectively. The Sauter mean diameter is the volume-weighted-to-area-weighted mean diameter that is useful for characterizing the optical properties of particles. The fits shown in Fig. 1 are to the most complete data sets given in Ref. 32 (Ref. 32, Fig. 13, $t = 13$ min). A less complete data set also given in this reference (Ref. 32, Fig. 12, $t = 7$ min) has a smaller exponent and puts a somewhat greater fraction of the surface area in the small particle mode.

Because there are no measurements of the particle size distributions of SRMs in the stratosphere for particles with diameters greater than 2 μm, we will infer the large particle distribution from ambient stratospheric particle measurements and the tropospheric STS plume particle measurements. A comprehensive analysis of ambient stratospheric particle data taken during the period of 1976–1984 was made by Zolensky et al.[44] All of these data were collected between an altitude of 17 and 19 km with NASA WB-57F and U2-C aircraft using retractable solid inertial impaction collectors. All samples were analyzed for morphology, size, and chemical composition. Approximately an order of magnitude increase in total large solid particle number density and a factor 20 increase of Al (particles containing aluminum and alumina components only) and Al′ (primarily aluminum with lesser amounts of other elements) particle number density of the stratosphere occurred during the study period. This increase is attributed to SRM exhaust and rocket and satellite debris. The main source of the Al and Al′ particles is rocket motor exhaust and ablating spacecraft. About half the 1984 Al particles are spherical and these spherical particles are attributed solely to SRM exhaust. If we assume that the spherical particle size distribution of the Al particles is not grossly different from that of the nonspherical Al distribution, then the particle size distribution of the 1984 data of Ref. 44 can be used to calculate estimated mean diameter of the large particles in the SRM plume. These data, plotted and fit to an exponential in Fig. 2, show a Sauter mean diameter equal to 4.1 μm and slope 0.73. The large-particle-size distributions of Space Shuttle plumes were measured in the troposphere at altitudes of 3 and 7 km and appeared to be independent of altitude.[36] The distribution measured at 3 km is also plotted and fit to an exponential in Fig. 2. It is clearly monomodal and has a Sauter mean diameter of 3.2 μm and slope of 0.86.

Because the ambient distribution plotted in Fig. 2 is due primarily to large SRM exhaust, and the tropospheric plume measurements did not change with altitude up to 7 km, one could argue that the stratospheric large-particle distribution has a mean diameter and slope between those shown in Fig. 2. Accordingly, we assume that the large-particle distribution has a Sauter mean diameter of 3.6 μm and a slope of 0.8. Note that this slope is more than twice the slope of the intermediate distribution given in Fig. 1, indicating a trimodal particle distribution for large SRMs in the stratosphere.

Stratospheric Plume Diameters and Expansion Rate

Plume Dispersion Data

A vital parameter required for the understanding of a SRM stratospheric plume is its dispersion rate. A rapidly expanding plume will quickly lower the particle densities (and chemical concentrations), making real-time detection difficult. Unfortunately, there is only one previous measurement of stratospheric SRM plume expansion. To increase the database, we infer plume size and expansion rate from the U-2 flythrough data of Strand et al.[32] and extract plume expansion rates from recently acquired videotapes of a Space Shuttle (STS) launch. All of these data measure expansion only during the first 10 min or so after vehicle passage, and the rates measured are an order of magnitude higher than those generally attributable to large-scale eddie diffusion. In this section, we review these data, review recent plume dispersion models, and compare the data to the models.

A search of the literature found only one observation of SRM plume expansion in the stratosphere. Hoshizaki[45] reported observations of the first few minutes of plume growth of an Oct. 4, 1974, launch from Vandenberg Air Force Base. Measurements were made from photographs of a large solid rocket booster (presumably a

Table 1 Plume-particle characteristics from model

Particle mode	Sauter mean diameter D_{32}, μm	Average particle density, ρ_{avg} g/cm^3	Mass fraction in particle model	C_m mass per volume air: peak value, g/cm^3	Number density: peak value, cm^{-3}	Total particle area per volume air: peak value, μm^2/cm^3
Small	0.056	4.0	0.012	2.0×10^{-12}	8.8×10^3	53
Medium	1.0	3.6	0.015	2.4×10^{-12}	7.94	6.7
Large	3.6	2.6	0.974	1.6×10^{-10}	6.16	125

Titan III) by Lockheed, under Contract to NASA Ames Research Center, using cameras located at four ground sites surrounding the launch pad. The photographs, taken of the plume for approximately 10 min, measure plume expansion between altitudes of 18 and 19 km. The data show a linear expansion rate of about 0.3 km/min.

As already noted, Strand et al.[32] obtained data on alumina particle density and size distribution in the stratosphere from two Titan IIIc launches (May 20, 1975, and June 8, 1975). Although their study did not address plume dispersion, information contained in their paper can be used to infer approximate early dispersion rates. On each of these launches, a U-2 aircraft made two traversals of the plume at times $T + 7$ and $T + 13$ min (May 20) and $T + 6.5$ and $T + 13.5$ min (June 5) at an altitude of 19 km. Measurements of total particle number densities at these respective times yielded values of 10^9 and 10^8 m^{-3} (May 20) and 10^{10} and 10^9 m^{-3} (June 6). The authors state that 10^{10} m^{-3} is the theoretically predicted value for the particle number density at early times. Thus, they find that the particle density decreases by an order of magnitude for a factor of two increase in plume expansion time. This rate of expansion is consistent with a plume expanding in three dimensions at a linear expansion rate or in two dimensions at an expansion rate of $t^{3/2}$. All data and most models show a linear expansion with time. All models assume two-dimensional expansion. As discussed in the Appendix, the individual density measurements of Strand et al.[32] varied between 60 and 100% of their true value depending on the ratio of the sample bag fill time to vehicle transit time through the plume. Within this accuracy range, these measurement are consistent with the other data and models.

An estimate of the cross-sectional area of the plume (and, hence, the diameter) can be obtained by dividing the mass flow rate of the Titan IIIc vehicle (16 g/cm of vehicle track at an altitude of 19 km) by the average mass density. The average mass density is given in Table 1 and was calculated from Eq. (14) to follow using the particle size distribution from Figs. 1 and 2, a density model for the alumina particles given by Eq. (15), an average value of the 10^{10} m^{-3} for the particle density at 600 s, and an exponential profile for the spatial distribution of the particles as will be explained. Averaging the mass over an area given by a radius defined by the distance required for the particle density to fall to e^{-2} of its peak value yields a diameter of 5 km. Using an averaging distance set by an e^{-1} density falloff yields a diameter closer to 4 km.

Additional information presented in Ref. 32 allows another estimate of the plume diameter to be made. The work notes that the time required to fly through the plume was between 5 and 10 s. This corresponds to a distance of 1–2 km because the speed of the U-2 is 200 m/s. Interpretating these distances as the plume diameters is complicated by several factors: the horizontally flying aircraft traversing a nonvertical plume will measure a distance greater than the diameter, traversing a cord will measure a distance smaller than the diameter, and the criterion for the detection of the edge of the plume is unidentified. Nevertheless, making this association yields an approximate plume diameter of 1.5 km. In summary, data from the U-2 flythroughs of a Titan III plume at an altitude of 19 km indicate a plume diameter between 1.5 and 5 km approximately 10 min after vehicle passage and are consistent with a two-dimensional linear (in time) expansion.

A recent video taken of a Titan IV launch (K-10, Feb. 7, 1994) presented the opportunity of estimating early plume diameters and expansion rates. This flight was launched from launch complex 41 (LC-41) from Kennedy Space Center and was observed from universal camera site 2 (UCS2), a distance of 7.6 km from LC-41. An infrared and a visible camera tracked the flight to 30 km ($T + 96$ s) and then held position to observe the plume. Additional details on the design of the infrared experiment are available.[16] The visible camera was used to estimate the diameter of the plume at an altitude of 30 km, and the analysis of its data is reported here. At $T + 96$ s, the surface distance from UCS2 to the rocket was 33.8 km, resulting in a 45.2 km range for the 30 km altitude. Thus, at this distance the rectangular field of view of the visible camera (0.14 rad horizontal, 0.11 rad vertical) was 6.6 km horizontal and 5.0 km vertical. The horizontal viewing angle was 11.6 deg off of alignment with the trajectory.

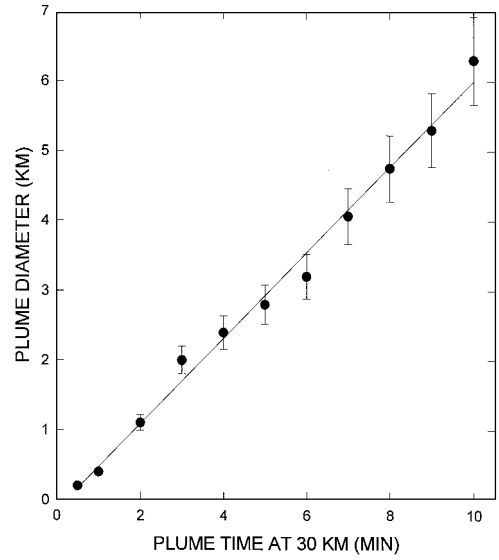

Fig. 3 Estimated plume diameter at an altitude of 30 km from the K-10 launch of a Titan IV; precision of the measurement of each estimated diameter is ± 10%.

The diameter of the plume was estimated by marking the 30-km altitude position on the video screen and observing the expansion of the plume in a direction normal to the centerline of the plume. The plume was observed to expand symmetrically around its centerline. After 4 min, the lower edge of the plume expanded off the bottom of the screen, and diameters were subsequently measured from the center of the expansion to the upper edge of the plume and doubled to obtain the diameter. Even though the day was clear, the plume was sufficiently dispersed to make it difficult to discern its edge after about 10 min. The estimated diameters are shown in Fig. 3. The diameter of the plume increases linearly with time at rate of approximately 0.6 km/min. The most relevant measurement of local wind conditions was at 6 a.m. local time, whereas the launch was in the late afternoon. At 6 a.m., the wind speed was 5.9 m/s from 182 deg at an altitude of 28 km.

Plume Dispersion Models

Three models of plume dispersion are reviewed. The first, by Watson et al.,[46] is believed to be accurate for times longer than a few hours after launch (>1 day). The second is the model[6] based on the data of Hoshizaki[45] and is thus verified for short times (10 min). The third model is by Ross[11] and is designed for times intermediate to these periods.

Watson et al.[46] made a study of Space Shuttle plume dispersion characteristics of F_2 and N_2O_4 in the stratosphere and mesosphere. Above an altitude of 100 km, plume dispersal is dominated by

molecular diffusion. Below this altitude, dispersion is produced by both small- and large-scale eddies that can be parameterized in terms of an overall eddy transport coefficient. Using a theoretical model (based on an admittedly limited database) previously developed,[47] Watson et al.[46] obtained a time scaling of the horizontal diffusion coefficient K_{yy} based on the model results at 100 km. At times less than 10^5 s, they state that this model may underestimate the horizontal plume dispersal rate due to an incorrect time evolution of K_{yy}.

The vertical dispersal (the main emphasis of Ref. 46) is two to three orders of magnitude less than this horizontal dispersal rate so that the expansion proceeds primarily in two dimensions. Watson et al.[46] used this model to calculate the plume width and densities at an altitude of 40 km at times of 0 s, 1 h, 5.6 h, 1 day, 10 days, and 1 month. Because of uncertainties of K_{yy}, they state that the calculations of plume volumes are only accurate to an order of magnitude. Their results indicate an initial expansion rate (0–1 h) of 1.4 km/h (0.023 km/min) and at longer times a nearly linear expansion rate of 5.2 km/h. Brady and Martin[7] used these values to scale temporal dependence of the chemical concentrations in the plume and found a time dependence (with t in seconds) of the concentration given by

$$n(t) = \frac{n_0}{1 + [(2 \times 10^{-3})t]^{2.6}} \tag{1}$$

where the initial value of n_0 was scaled with local atmospheric pressure.

In their chemical model calculating local ozone depletion by solid rocket plumes, Denison et al.[6] modeled the diffusion of the plume by solving the conservation equation in cylindrical coordinates,

$$\frac{\partial n}{\partial t} = K_{yy}\nabla^2 n = \frac{1}{r}\frac{\partial}{\partial r} r K_{yy}\frac{\partial n}{\partial r} \tag{2}$$

where n is the number density, r is the radial coordinate, t is time, and K_{yy} is the horizontal diffusion coefficient. Using the plume size measurements of Hoshizaki[45] taken at an altitude of 18 km, they found the diffusivity to be scale dependent, where

$$K_{yy} = br \tag{3}$$

and $b = 1.75$ m s^{-1}. Under this assumption, the solution of Eq. (2) for a line source is

$$n(r, t) = At^{-2}\exp(-r/bt) \tag{4}$$

where A is a normalization constant. We write this solution as

$$n(r, t) = n_0(t_0/t)^2\exp\{-(1/b)[(r/t) - (r_0/t_0)]\} \tag{5}$$

where n_0 is the particle number density at r_0 and t_0. If $r_0 = 0$, then n_0 is the peak (centerline) number density. Using the relation

$$\frac{n[R(t), t]}{n[R_i, t]} = e^{-2} \tag{6}$$

to define the radius of the plume, we find that the time dependence of the plume radius is

$$R(t) = R_i + 2bt \tag{7}$$

where R_i is the initial radius. Assuming $R_i = 5$ m, the plume diameters at 1 and 10 min are 430 m and 4.2 km, respectively. This diffusion model was also employed by Kruger[5] and by Brady and Martin[7] to calculate the local stratospheric ozone depletion by a solid rocket in their chemical kinetics models.

More recently, Ross[11] completed a model of a Titan IV SRM plume in the atmosphere that included a limited chemical reaction set and fluid dynamic mixing in the stratosphere for up to 8 h after launch. The model assumes cylindrical symmetry in a series of 1-km-thick layers and builds a three-dimensional model by permitting the layers to move independently according to their altitude-dependent zonal (E–W) and meridional (N–S) wind speeds. This model also parameterizes the transport in terms of an eddy diffusion coefficient using a time-dependent value of K_{yy} (m^2 s^{-1}) = $0.01t$ (s)$^{1.3}$, a value assumed to be independent of altitude. This work presents Al_2O_3 number densities at $T + 1.25$ h and $T + 4.25$ h for altitudes of 20, 30, and 40 km. Defining a radius at the $1/e^2$ density, the diameters inferred from the density plots of this model are given in Table 2. These values indicate an expansion rate of about 3 km/h.

Table 2 Plume diameters calculated from Ref. 11

Alt, km	$T + 1.25$ h	$T + 4.25$ h
20	2.8	12
30	2.4	10
40	4.0	——

Expansion Rate Data: Model Comparison

It is useful to compare the data of the early plume expansion with the dispersion models being employed by the plume chemistry models. Because the data were taken at different altitudes, this comparison requires some understanding of the altitude scaling of the small-scale eddy diffusion coefficient. Unfortunately, there are no studies of the scaling of this parameter with altitude. The large-scale atmospheric eddy diffusion coefficient, however, has received considerable study for the purposes of global atmospheric modeling. The scaling of the large vertical eddy diffusion coefficient K_{zz} with altitude between 18 and 40 km varies from being constant to increases of a factor of 25 (varying approximately with inverse atmospheric pressure) depending on the model.[46,48,49] Plots of the variation of large-scale K_{yy} as a function of altitude and latitude are given in Ref. 46, which were taken from Ref. 48. At a latitude of 30 deg, there is little variation of this parameter in the 20–40 km altitude range. Based on the data presented by Hoshizaki,[45] Denison et al.[6] found that the small-scale values of K_{yy} at 10 min are two to three orders of magnitude smaller than those of the large-scale values. If the early linear growth rate continues unabated, 1–2 days are required before the values of the small-scale diffusivity reach the large-scale values. Therefore, the applicability of these large-scale altitude variations of K_{yy} and K_{zz} to the small scale values of K_{yy} is highly questionable, and the small-scale altitude variation must be considered unknown at this time.

Tropospheric measurements of the small-scale K_{yy} values at altitudes between 2 and 4 km of a nuclear debris cloud give values similar to ($\cong 1000$ m^2/s) the stratospheric values noted here.[50] Given the large differences between the troposphere and the stratosphere, this must be taken as evidence that the altitude variation of small-scale K_{yy} is not large. A very conservative approach to altitude scaling is to consider the initial value of the plume diameter to be a function of the local atmospheric pressure. This pressure, which can be approximated by $p(z) = 1222\exp(-0.155z)$ mbar (z in kilometers) decreases from 55 mbar at 20 km to 2.5 mbar at 40 km. Zittel[8] finds that the afterburning exhausting gases cool and expand to near-ambient conditions within a few seconds of entering in the stratosphere. He also finds that the diameter of the plume is approximately 50 m at an altitude of 20 km in these first few seconds. Because the ambient temperature is constant within 15% throughout the stratosphere, one expects that this initial plume diameter will scale as $p(z)^{-1/2}$, creating an initial diameter of about 80 m at an altitude of 20 km and 300 m at 30 km. Then, following Eqs. (3) and (7),

$$K_{yy}(z) = b[R_i(z) + 2bt] \tag{8}$$

where

$$R_i(z) = \left[\frac{p(z_0)}{p(z)}\right]^{\frac{1}{2}} R_{i0} \tag{9}$$

where R_{i0} is the initial reference radius of the Titan plume at the nozzle exit plane ($\approx$25 m at an altitude of 20 km). This scaling affects the plume diameters only at the earliest times and is negligible at all measurement times.

Table 3 compares the measured and model values. Also included in Table 3 is the estimated diameter of the Titan III plume about 12

Table 3 Diffusion data-model comparison

	Data				Diffusion models				
Characteristic	Titan III[14]	Hoshizaki[45]	Strand et al.[32]	Titan IV K-10	Watson et al.[46]	Denison et al.[6]		Ross[11]	
Altitude, km	18	18	19	30	alt. indep.	alt. indep.	20	30	40
D, km, at 10 min	3.0	3.0	1.5–5	6.0	0.23	4.2	0.5	0.4	0.67
Expansion rate, km/h		18	9–30	36	1.4	25	2.9	2.4	4.0
Chemistry model using diffusion model		Ref. 2			Ref. 7	Refs. 2, 4, 7		Ref. 8	

min after vehicle passage mentioned in Ref. 14. Given the large variability of climate that can affect plume expansion rates, the agreement among the observed values must be considered remarkable. The models show considerably less agreement among their values. The Watson et al.[46] model predicts the smallest value for the 10-min diameter. This disagreement is not surprising inasmuch as the model was designed for long times, and the authors speculate that their model may underpredict the initial diameters. The predictions of the Ross[11] model are a factor of two greater than the Watson et al.[46] model but are still an order of magnitude below the predictions of the model of Ref. 6. The model of Denison et al.[6] most closely reproduces the observed diameters, which is not surprising given that its diffusion coefficient is based on the Hoshizaki[45] data.

Table 3 also indicates the diffusion models used as inputs to the models of stratospheric plume chemistry. Chemical models using the diffusion model of Ref. 46 will predict chemical concentrations that are too large at early times. The dispersion at long times is best approximated by this model, after the eddy diffusion lengths have reached meteorological scales of hundreds of kilometers. It may require a day or more for the diffusion to reach this size. The model of Denison et al.[6] should be the most accurate at short times and will result in chemical concentrations that are less than those predicted by Refs. 7 and 11. Because several of the chemical reaction rates depend quadratically on chemical concentration, the chemistry will depend quite severely on this initial expansion rate. Indeed, this dependence has been modeled by Ref. 7, showing that the size and persistence of the ozone hole depend on the dispersion rate, peaking for the rate chosen for their work. Accordingly, the size and persistence of the predicted local ozone depletion by all of the plume chemistry models depend critically on the initial plume dispersion rate. Because all instruments under consideration for verifying ozone chemistry models of the plume are designed to operate in the first several hours, they should use models that employ the early plume dispersion rates.

Model for the Specific Particle Density

Based on this discussion, we present a model for the specific density of particles (number/air volume/particle diameter) for an SRM plume as a function of position and time. In this model, we assume that the particle density is a smoothly varying, cylindrically symmetric function. This is obviously an oversimplification as any visual observation of the expanding plume will show. Nevertheless, for the purposes of line-of-sight observations through the plume and measurements or calculations time averaged over a time interval, this convenient approximation is useful. The radial and temporal dependence is taken from the solution of the conservation equation for a line source and a scale-dependent diffusivity. The functional dependence on the particle diameter is assumed to be exponential following the analysis of the experimental data presented in Figs. 1 and 2. Then for a single-mode particle-size distribution, we write

$$n_D(D, r, z, t) \equiv \frac{\mathrm{d}n(D, r, z, t)}{\mathrm{d}D} = n_{D0}(z)\left(\frac{t_0}{t}\right)^2 \exp\left[\frac{-r}{b(z)t}\right]\exp[-\gamma(z)D] \quad (10)$$

where D is the particle diameter and the time dependence of normalization parameter $n_0(z)$ is factored out to give $n_0(z)$ the intuitive dimensions of specific density. In general, the parameters $n_0(z)$, $b(z)$, and $\gamma(z)$ are altitude dependent. Certainly, the initial value of the plume diameter, and hence its particle density, is a function of the local atmospheric pressure. As noted, this initial diameter is small. The line-source solution of the conservation equation assumes a negligible initial plume diameter. Because these diameters are small compared to the observed plume diameters after a minute or two of expansion, this solution is a good approximation after a few minutes, and this altitude dependence will be ignored. Also as discussed, the altitude variation of $b(z)$ is unknown but the limited data available suggest that its dependence on altitude is small. Accordingly, we will consider this parameter to be independent of altitude. Finally, available evidence suggests that the particle size mode parameter γ is independent of altitude.[36]

The particle size distribution is assumed to be trimodal. The small- and medium-size distributions are given by those shown by the fits in Fig. 1. The large particle distribution is given by the intermediate fit values inferred from the curves in Fig. 2, constrained to give the same density value at 1 μm as that of the medium-diameter particles in Fig. 1. Generalizing Eq. (10) to an expression for trimodal distribution is done by a straightforward summation of the (assumed) independent number densities of each distribution. Each mode has a different initial spatial distribution. The small particles ($< 0.25\ \mu$m) readily follow propellant gas through the rocket nozzle and thus are evenly distributed across the diameter of the plume. Particles greater than 1 μm in diameter do not follow the flow and are confined to the central core of the plume. Given the turbulent mixing that takes place in an afterburning plume, it is unrealistic to assume that particle size radial segregation has any physical meaning in a realistic plume. Thus, we consider the particle size modes are spatially mixed and assume that the expansion rates of each of the three modes are equal.

We define the region for averaging the particle density over the assumed exponential spatial distribution to be the radius where the number density falls to e^{-2} of its peak value. This averaging is used to obtain the peak particle number densities for the three modes. The normalization procedure is discussed in the Appendix, and it yields

$$n_D(D, r, t) = \left(\frac{t_n}{t}\right)^2 \exp\left(-\frac{r}{bt}\right)\sum_{i=1}^{3} n_i \exp(-\gamma_i D) \quad (11)$$

where

$$n_1 = 8.3 \times 10^{12} \qquad \gamma_1 = 63.3$$
$$n_2 = 1.8 \times 10^{8} \qquad \gamma_2 = 3.13$$
$$n_3 = 3.3 \times 10^{7} \qquad \gamma_3 = 0.80$$

and the n_i are $\mathrm{m}^{-3}\mu\mathrm{m}^{-1}$ and the γ_i are $\mu\mathrm{m}^{-1}$. The normalization time is $t_n = 344$ s, and the summation is over the three particle size modes. This model predicts particle size distribution and density of plumes of a Titan IV vehicle in the 18–40 km range during its early expansion. The model can be used for other SRMs by scaling the mass exhaust rate and the vehicle velocity to those of the Titan IV. For example, the STS (Shuttle) and the Titan III have similar velocity profiles. Thus, one only has to multiply the right-hand side of Eq. (11) by the ratio of the mass flow rates (0.87 for the Titan III and 1.66 for the STS) to obtain the particle density for these vehicles.

Predicted Physical Characteristics of SRM Exhaust Based on Model

The physical properties of the plume due to the particles can be readily calculated using the particle model. The total number density $n(r, t)$, the total area of all particles per volume of air a_{tot}, and the mass per volume of air C_m are given, respectively, by

$$n(r, t) = \int_0^\infty n_D(D, r, t)\, \mathrm{d}D \tag{12}$$

$$a_{\text{tot}}(r, t) = \int_0^\infty n_D(D, r, t) A(D)\, \mathrm{d}D \tag{13}$$

$$C_m(r, t) = \int n_D(D, r, t) \rho(D) V(D)\, \mathrm{d}D \tag{14}$$

where $n_D(D, r, t)$ is given by Eq. (11). The surface area of a particle, $A(D) = \pi D^2$, and the volume of a particle, $V(D) = \pi D^3/6$, are assumed to be time independent. As noted, the particle density varies with particle size. For this, we choose a model of density that varies exponentially with particle diameter, namely,

$$\rho(D) = 1.65 + 2.4 \times 10^{-0.195D} \tag{15}$$

with D in micrometers and ρ in grams per cubic centimeter. This function yields a density of 1.7 g/cm^3 at a particle diameter of 10 μm, 4.0 g/cm^3 at 0.01 μm, and reasonable intermediate values.

Equations (12–14) can be evaluated separately for each of the three modes. Caution must be exercised when calculating size properties (diameter, surface area, volume, mass, etc.) using exponential particle size distributions. Physical distributions are not exponential on the low and high ends of the size parameter. Mugele and Evens[51] show that fitting exponential functions to size histograms can predict erroneous size properties if the distributions are not properly truncated. They introduce an upper-limit distribution function (ULDF) that limits the largest particle size to a specified finite diameter. The ULDF is written in terms of two additional parameters that do not lend themselves to direct geometrical interpretations (see, for example, Ref. 52). There are only four data points in each of the two modes in Fig. 1, and fitting a three-parameter ULDF to these few points does not yield well-defined parameters. Accordingly, it was decided to retain the exponential fits shown in Figs. 1 and 2 and set the limits of integration to the values of the smallest and largest diameters measured.

Peak values ($r = 0$) for these quantities at $t = 600$ s are shown in Table 1. The peak values can be converted to values spatially averaged over a diameter defined by the distance required for the number density to drop to e^{-2} of its peak value by multiplying the peak value by 0.43 (see the Appendix). Decreasing the lower limit of integration to zero in the small mode increases the area percentage in this mode by about 5%. Increasing the large mode integration limit to 100 μm increases the large mode area percentage by about 1%.

Examination of Table 1 shows that nearly all of the mass is in the large particles but the small particle number density is much greater than the number density of large particles, as expected. The total surface area available for the heterogeneous reactions resides mostly in the large particles even though the small particles offer much greater surface area on a per mass basis. Because both the small- and large-mode particles contribute comparable surface areas, this area should be measured for both modes. The large-particle surface area is more amenable to measurement by transmission techniques because it has a large attenuation coefficient.[25]

Summary and Conclusions

This work presents a unified model for the particle size distribution, particle density, and geometrical dispersion for the alumina particles in the exhaust of an SRM plume in the stratosphere. Although the model is based on the best available measurements, there are serious gaps in the database, especially in the dispersion rates of the plume after the first 10 min. The particle size distribution is trimodal with nearly all of the particles in the small-size mode but with nearly all the mass in the large-size mode. About two-thirds of the particle surface area available for heterogeneous chemical reactions is due to the large-particle mode whereas most of the remaining surface area is due to the small-particle mode. These results are useful for designing instruments required to measure the chemical and physical properties of the SRM plume and predicting the effect of particles from the plume on heterogeneous stratospheric ozone chemistry.

Appendix: Normalization of the Particle Density Distribution

The spatial and temporal development of the density is based on the line solution of the conservation equation with a size-dependent diffusion parameter. The functional form can be expressed in the form given by Eq. (11). To normalize, the size distribution is first converted to a density

$$n(r, z, t) = \int_{D_{\min}}^{D_{\max}} n_D(D, r, z, t)\, \mathrm{d}D = \left(\frac{t_c}{t}\right)^2 \exp\left(\frac{r_c}{bt_c}\right) \sum_{i=1}^{3} a_i n_i \exp\left[-\frac{r_i(t, z)}{bt}\right] \tag{A1}$$

where coefficients a_i are obtained from the integration over the particle size distributions,

$$a_1 = \int_{0.025}^{0.244} e^{-b_1 D}\, \mathrm{d}D = 3.2 \times 10^{-3} \tag{A2}$$

$$a_2 = \int_{0.245}^{0.99} e^{-b_2 D}\, \mathrm{d}D = 0.13 \qquad a_3 = \int_{1.0}^{10} e^{-b_3 D}\, \mathrm{d}D = 0.57$$

Then this spatial distribution is averaged and set equal to the average density measured by Strand et al.[32]:

$$\overline{n(z, t)} = \left(\frac{t_c}{t}\right)^2 \exp\left(\frac{r_c}{bt_c}\right) \sum_{i=1}^{3} n_i \overline{\exp\left[-\frac{r_i(t, z)}{bt}\right]} a_i \tag{A3}$$

$$\overline{n(z, t)} = c \left(\frac{t_c}{t}\right)^2 \exp\left(\frac{r_c}{bt_c}\right) \sum_{i=1}^{3} n_i a_i \tag{A4}$$

where $\overline{n(z = 19\text{ km},\ t = 344\text{ s})} = 1.14 \times 10^{10}$ m^{-3} (converting from a Titan IIIc to a Titan IV density) and $c = 0.43$ for an average over a radius were the density drops to e^{-2} of its peak value. Finally, setting $z_c = 19$ km, $t_c = 344$ s, $r_c = 2$ km, $b = 1.75$ m/s, and noting $n_1/n_2 = 4.65 \times 10^4$ (from fits on Fig. 1) and $n_2/n_3 = 10.3$ (from requiring lower fit on Fig. 1 and median fit of Fig. 2 to have the same value at $D = 1$ μm), we find

$$n_1 = 0.16 \qquad n_2 = 3.5 \times 10^{-6} \qquad n_3 = 3.3 \times 10^{-7} \tag{A5}$$

Note that the absolute density of this model relies on the density measurement of Strand et al.[32] This measurement was made using an electrical mobility analyzer (EMA). The EMAs were calibrated against a standard at the factory and corrected for operation in the low-pressure operation in the instrument bay of the ER-2. The EMAs measured the densities in the range of 0.03–1 μm and give absolute concentrations when the sampling time is shorter than the transit time through the plume. To fill the EMA sample bag 3–8 s were required, and to traverse the early contrail 5–10 s were required. Thus, the EMA could underestimate the density by mixing air from outside the plume into the same volume. Whether this was taken into consideration by these workers[32] in the values reported is not known, but the value of 10^4 cm^{-3} is the highest value they reported, and these authors stated that this value was consistent with predicted values.

Acknowledgments

This work was supported by the Environmental Management Division, U.S. Air Force HQ SMC/CEV, and coordinated by the Environmental Programs Office of The Aerospace Corporation under Contract F04701-93-C-0094. The author thanks J. A. Syage for useful discussions on light detection and ranging (LIDAR) and total ozone mapping spectrometer (TOMS) measurements, B. B. Brady and L. R. Martin for information and discussions on their plume model, J. T. Knudson for making the video tape of the K-10 available and (with D. R. Schulthess) providing information on the K-10 launch, and M. R. Denison for information of the altitude scaling of the small-scale eddy diffusion coefficient.

References

[1]Brady, B. B., Fournier, E. W., Martin, L. R., and Cohen, R. B., "Stratospheric Ozone Reactive Chemicals Generated by Space Launches Worldwide," The Aerospace Corp., TR-94(4231)-6, El Segundo, CA, Sept. 1994.

[2]"Scientific Assessment of Ozone Depletion: 1991," World Meteorological Organization Global Ozone Research and Monitoring Project, Rept. 25, Ozone Secretariat, Geneva 20, Switzerland, 1991.

[3]Jackman, C. H., Considine, D. B., and Fleming, E. L., "Space Shuttle's Impact on the Stratosphere: An Update," *Journal of Geophysical Research*, Vol. 101, No. D7, 1996, pp. 12,523–12,529.

[4]Kruger, B. C., Hirschberg, M. M., and Fabian, P., "Effect of Solid-Fueled Rocket Exhausts on the Stratospheric Ozone Layer," *Berichte der Bunsengesellschaft für Physikalrsche Chemic*, Vol. 96, 1992, pp. 268–272.

[5]Kruger, B. C., "Ozone Depletion in the Plume of a Solid-Fuel Rocket," *Annales Geophysicae,* Vol. 12, No. 3, 1994, pp. 409–416.

[6]Denison, M. R., Lamb, J. J., Bjorndahl, W. D., Wong, E. Y., and Lohn, P. D., "Solid Rocket Exhaust in the Stratosphere: Plume Diffusion and Chemical Reactions,"*Journal of Spacecraft and Rockets*, Vol. 31, No. 3, 1994, pp. 435–442.

[7]Brady, B. B., and Martin, L. R., "Modeling Solid Rocket Booster Exhaust Plumes in the Stratosphere with SURFACE CHEMKIN," The Aerospace Corp., TR-95(5231)-9, El Segundo, CA, Sept. 1995.

[8]Zittel, P. F., "Local Effects of Large, Solid Rocket Motors on Stratospheric Ozone," The Aerospace Corp., ATR-92(9558)-2, El Segundo, CA, Aug. 1992.

[9]Zittel, P. F., "Computer Model Predictions of the Local Effects of Large, Solid-Fuel Rocket Motors on Stratospheric Ozone," The Aerospace Corp., TR-94(4231)-9, El Segundo, CA, Sept. 1994.

[10]Ross, M., "Potential Impact of Solid Rocket Motor Exhaust on Stratospheric Ozone," The Aerospace Corp., TOR-92(2562)-2, El Segundo, CA, 1992.

[11]Ross, M., "Local Impact of Large Solid Rocket Motor Exhaust on the Stratospheric Ozone and Surface Ultraviolet Flux," *Journal of Spacecraft and Rockets,* Vol. 33, No. 1, 1996, pp. 144–153.

[12]Martin, L. R., "Possible Effect of the Chlorine Oxide Dimer on Transient Ozone Loss in Rocket Plumes," The Aerospace Corp., TR-94(4231)-1, El Segundo, CA, March 1994.

[13]TRW Space and Electronics Group, and Prather, M. J., "The Impact of Tropospheric Rocket Exhaust on Stratospheric Ozone," TRW/UCI, El Segundo, CA, May 1994.

[14]Pergament, H. S., Gomberg, R. I., and Poppoff, I. G., "NO_x Deposition in the Stratosphere from the Space Shuttle Rocket Motors," NASA TM Z-58198, G-3, Appendix G, Jan. 1977.

[15]McKenzie, D. L., Gutierrez, D. J., Hecht, J. H., Marbry, D. J., Ross, M. N., Tossano, G. S., Sivjee, M. G., and Stein, J. A., "System Requirements Review for the High-Resolution Ozone Imager (HIROIG)," The Aerospace Corp., TR-93(4231)-9, El Segundo, CA, Sept. 1993.

[16]Knudtson, J. T., Hall, J. T., Stone, D. K., Koffend, J. B., Schere, G. J., Foster, K. L., Heidner, R. F., and Herr, K. C., "Ground Based Infrared Monitoring of Stratospheric Ozone Impacts Due to Solid Rocket Boosters," The Aerospace Corp., TOR-94(4230)-1, El Segundo, CA, Dec. 1993.

[17]Zittel, P. F., "A Computer Modeling Study of Passive IR Detection of HCl Afterburing in Titan IV SRM Plumes," The Aerospace Corp., TOR-94(4230)-2, El Segundo, CA, April 1994.

[18]Syage, J. A., and Ross, M. N., "An Assessment of the Total Ozone Mapping Spectrometer for Measuring Ozone Levels in a Solid Rocket Plume," *Geophysical Research Letters*, Vol. 23, No. 22, 1996, pp. 3227–3230.

[19]Syage, J. A., "Direct Absorption Spectroscopy of a Solid Rocket Plume," The Aerospace Corp., TOR-95(5231)-1, El Segundo, CA, April 1995.

[20]Whitefield, P. D., Hagen, D. E., and Hopkins, A. R., "Rocket Impact on Stratospheric Ozone: Submicron Aerosol Measurement," AIAA Paper 97-0529, Jan. 1997.

[21]Dao, P., Gelbwachs, J. A., Farley, R., Garner, R., Soletsky, P., and Davidson, G., "LIDAR Stratospheric Solid Rocket Motor Exhaust Plume Measurments," AIAA Paper 97-0526, Jan. 1997.

[22]Hanning-Lee, M. A., Brady, B. B., Martin, L. R., and Syage, J. A., "Ozone Decomposition on Alumina: Implications for Solid Rocket Motor Exhaust," *Geophysical Research Letters,* Vol. 23, No. 15, 1996, pp. 1961–1964.

[23]Syage, J. A., "The Impact of Heterogeneous Chemistry on Alumina to Global Stratospheric Ozone," *Journal of Physical Chemistry* (to be published).

[24]Meads, R., Spenser, D., and Molina, M., "Stratospheric Chemistry of Aluminium Oxide Particles," TRW/MIT, El Segundo, CA, June 1994.

[25]Beiting, E. J., "Predicted Optical Characteristics of Solid Rocket Motor Exhaust in the Stratosphere," *Journal of Spacecraft and Rockets*, Vol. 34, No. 3, 1997, pp. 311–317.

[26]Youngborg, E. D., Pruitt, T. E., Smith, M. J., and Netzer, D. W., "Light-Diffraction Particle Size Measurements in Small Solid-Propellant Rockets," *Journal of Propulsion and Power,* Vol. 26, No. 3, 1990, pp. 243–249.

[27]Brennan, W. D., Hovland, D. L., and Netzer, D. W., "Measured Particulate Behavior in a Subscale Solid Propellant Rocket Motor,"*Journal of Propulsion and Power,* Vol. 8, No. 5, 1992, pp. 954–960.

[28]Laredo, D., and Netzer, D. W., "The Dominant Effect of Alumina on Nearfield Plume Radiation," *Journal of Quantitative Spectroscopy and Radiative Transfer,* Vol. 50, No. 5, 1993, pp. 511–530.

[29]Kim, H. O., Laredo, D., and Netzer, D. W., "Measurement of Submicrometer Al_2O_3 Particle in Plumes," *Applied Optics*, Vol. 32, No. 33, 1993, pp. 6834–6840.

[30]Laredo, D., McCrorie, J. C., II, Vaughn, J. K., and Netzer, D. W., "Motor and Plume Particle Size Measurements in Solid Propellant Micromotors," *Journal of Propulsion and Power,* Vol. 10, No. 3, 1994, pp. 410–418.

[31]Radke, L. F., Hobbs, P. V., and Hegg, D. A., "Aerosols and Trace Gases in the Effluents Produced by the Launch of Large Liquid- and Solid-Fueled Rockets," *Journal of Applied Meteorology,* Vol. 21, No. 9, 1982, pp. 1312–1345.

[32]Strand, L. D., Bowyer, J. M., Varsi, G., Laue, E. G., and Gauldin, R., "Characteristics of Particles in the Exhaust Plume of Large Solid-Propellant Rockets," *Journal of Spacecraft and Rockets,* Vol. 18, No. 4, 1984, pp. 297–305.

[33]Cofer, W. R., III, Purgold, G. C., Edahl, R. A., and Winstead, E. L., "Solid Propellant Exhausted Aluminum Oxide and Hydrogen Chloride: Environmental Considerations," AIAA Paper 93-0305, Jan. 1993.

[34]Cofer, W. R., III, Bendura, R. J., Sebacher, D. I., Pellett, G. L., Gregory, G. L., and Maddrea, G. L., "Airborne Measurements of Space Shuttle Exhaust Constituents," *AIAA Journal,* Vol. 23, No. 2, 1985, pp. 283–287.

[35]Cofer, W. R., III, Lala, G. G., and Wightman, J. P., "Analysis of Mid-Tropospheric Space Shuttle Exhausted Aluminum Oxide Particles," *Atmospheric Environment*, Vol. 21, No. 5, 1987, pp. 1187–1196.

[36]Cofer, W. R., III, Purgold, G. C., Winstead, E. L., and Edahl, R. A., "Space Shuttle Exhausted Aluminum Oxide," *Journal of Geophysical Research*, Vol. 96, No. D9, 1991, pp. 17,371–17,376.

[37]Cofer, W. R., III, Winstead, E. L., and Key, L. E., "Surface Composition of Solid-Rocket Exhausted Aluminum Oxide Particles," *Journal of Propulsion,* Vol. 5, No. 6, 1989, pp. 674–677.

[38]Dill, K. M., Reed, R. A., Calia, V. S., and Schultz, R. J., "Analysis of Crystalline Phase Aluminum Oxide Particles from Solid Propellant Exhausts," *Journal of Propulsion and Power,* Vol. 6, No. 5, 1990, pp. 668–671.

[39]Turco, R. P., Toon, O. B., Whitten, R. C., and Cicerone, R. J., "Space Shuttle Ice Nuclei," *Nature,* Vol. 298, Aug. 1982, pp. 830–832.

[40]Turco, R. P., Toon, O. B., Pollark, J. B., Whitten, R. C., Poppoff, I. G., and Hamill, P., "Stratospheric Aerosol Modification by Supersonic Transport and Space Shuttle Operations—Climate Implications," *Journal of Applied Meteorology,* Vol. 19, Jan. 1980, pp. 78–89.

[41]Dobbins, R. A., and Strand, L. D., "A Comparison of Two Methods of Measuring Particle Size of Al_2O_3 Produced by a Small Rocket Motor," *AIAA Journal*, Vol. 8, No. 9, 1970, pp. 1544–1550.

[42]Hwang, C. J., and Chang, G. C., "Numerical Study of Gas-Particle Flow in a Solid Rocket Nozzle," *AIAA Journal,* Vol. 26, No. 6, 1988, pp. 682–689.

[43]Dash, S. M., "Analysis of Exhaust Plumes and Their Interaction with Missile Airframes," *Tactical Missile Aerodynamics,* edited by M. J. Hemsch and J. N. Nielsen, Vol. 104, Progress in Astronautics and Aeronautics, AIAA, New York, 1986, pp. 778–851.

[44]Zolensky, M. E., McKay, D. S., and Kaczor, L. A., "A Tenfold Increase in the Abundance of Large Solid Particles in the Stratosphere as Measured over the Period 1976–1984," *Journal of Geophysical Research,* Vol. 94, No. D1, 1989, pp. 1047–1056.

[45]Hoshizaki, H., "Aircraft Wake Microscale Phenomena," *The Stratosphere Perturbed by Propulsion Effluents,* edited by G. D. Robinson, H. Hidalgo, and N. Sundararaman, Vol. 4, Climatic Impact Assessment Program Monograph Series, U.S. Dept. of Transportation Rept. DOT-TST-75-53, Washington, DC, 1975, Chap. 2, pp. 60–73.

[46]Watson, R. T., Smokler, P. E., and DeMore, W. B., "An Assessment of an F_2 or N_2O_4 Atmospheric Injection from an Aborted Space Shuttle Mission," Jet Propulsion Lab., Publication 77-81, California Inst. of Technology, Pasadena, CA, April 1978.

[47]Bauer, E., "Introduction and Overview: The Stratosphere in Its Application to Climatic Impact Assessment Program," Climatic Impact Assessment Program Monograph 1, The National Stratosphere of 1974, Dept. of Transportation Rept. DOT-TST-75-51, Washington, DC, 1975.

[48]Louis, J. F., "Two-Dimensional Transport Model of the Atmosphere," Thesis, Univ. of Colorado, Boulder, CO, 1974.

[49]Rowland, F. S., and Molina, M. J., "Chlorofluoromethanes in the Environment," *Review of Geophysical Space Physics*, Vol. 13, No. 1, 1975, pp. 1–35.

[50]Randerson, D., "Temporal Change in the Horizontal Diffusion Parameter of a Single Nuclear Debris Cloud," *Journal of Applied Meteorology,* Vol. 11, June 1972, pp. 670–673.

[51]Mugele, R. A., and Evans, H. D., "Droplet Size Distributions in Sprays," *Industrial and Engineering Chemistry*, Vol. 43, No. 6, 1951, pp. 1317–1324.

[52]Dobbins, R. A., Crocco, L., and Glassman, I., "Measurement of Mean Particle Sizes in Sprays from Diffractively Scattered Light," *AIAA Journal,* Vol. 1, No. 8, 1963, pp. 1882–1886.

I. D. Boyd
Associate Editor